

## Pressure Coefficient and Phase Diagram of He<sup>4</sup> near the Upper Lambda Point\*

HENRY A. KIERSTEAD

*Argonne National Laboratory, Argonne, Illinois*

(Received 26 January 1965)

Measurements are reported of the derivatives  $(dP/dT)_\lambda$ ,  $(d\rho/dT)_\lambda$ , and  $(d\rho/dP)_\lambda$  on the lambda curve, of  $(dP/dT)_m$  on the melting curve, and of the pressure coefficient  $\beta_v = (\partial P/\partial T)_v$  of the liquid very close to the upper lambda point  $(T_{\lambda'}, P_{\lambda'}, V_{\lambda'})$ . The measurements are well represented by the equations

$$\begin{aligned} (dP/dT)_\lambda &= -55.54 - 96(T_\lambda - T_{\lambda'}), & T_\lambda - T_{\lambda'} &\leq 12.5 \times 10^{-3} \text{ }^\circ\text{K}; \\ (d\rho/dT)_\lambda &= -43.7 - 230(T_\lambda - T_{\lambda'}), & T_\lambda - T_{\lambda'} &\leq 12.5 \times 10^{-3} \text{ }^\circ\text{K}; \\ (d\rho/dP)_\lambda &= 0.7868 + 2.8(T_\lambda - T_{\lambda'}), & T_\lambda - T_{\lambda'} &\leq 12.5 \times 10^{-3} \text{ }^\circ\text{K}; \\ (dP/dT)_m &= 29.43 + 326(T_m - T_{\lambda'}), & 0 &\leq T_{\lambda'} - T_m < 17 \times 10^{-3} \text{ }^\circ\text{K}; \\ (\partial P/\partial T)_v &= 9.39 + 7.69 \log_{10}(T - T_\lambda), & V &= V_{\lambda'}, \quad 6 \times 10^{-5} \text{ }^\circ\text{K} \leq T - T_\lambda \leq 6 \times 10^{-3} \text{ }^\circ\text{K}; \end{aligned}$$

where  $P$  is in atm,  $T$  is in  $^\circ\text{K}$ , and  $\rho$  is in  $\text{mg}/\text{cm}^3$ . The temperature and pressure of the upper lambda point are

$$T_{\lambda'} = 1.7633 \pm 0.0001 \text{ }^\circ\text{K}, \quad P_{\lambda'} = 29.84 \pm 0.02 \text{ atm.}$$

There is no evidence of a first-order transition in the solid in the temperature range  $-17 \times 10^{-3} \text{ }^\circ\text{K} < T - T_{\lambda'} < 4.3 \times 10^{-3} \text{ }^\circ\text{K}$ .

### INTRODUCTION

THE thermodynamics of the lambda transition in liquid He<sup>4</sup> can be investigated most advantageously close to the melting curve, where the anomalous behavior of the thermodynamic properties is spread out over a larger temperature interval than it is at lower pressures. For example, Lounasmaa,<sup>1</sup> working at  $P = 13$  atm, found that at a temperature  $T$  which was only  $2 \times 10^{-5} \text{ }^\circ\text{K}$  from the lambda point  $T_\lambda$ , the value of  $\beta_v = (\partial P/\partial T)_v$  was less than a fifth of its limiting value,  $(dP/dT)_\lambda$ . In the work to be reported at  $P = 29.8$  atm, we found that  $\beta_v$  was already nearly half of  $(dP/dT)_\lambda$  at  $T - T_\lambda = 10^{-4} \text{ }^\circ\text{K}$ . Another point of interest in this region of the phase diagram is the upper triple point, where the  $\alpha$ - $\gamma$  solid-phase-transition line meets the melting curve. The upper triple point has been reported<sup>2-4</sup> to be a few millidegrees above the upper lambda point  $T_{\lambda'}$ , where the lambda curve meets the melting curve. We have accordingly studied the melting curve, the lambda curve, and an isochore, all in the region near the upper lambda point, with an apparatus designed to measure derivatives directly. The resolution was  $10^{-6} \text{ }^\circ\text{K}$  in temperature,  $10^{-6}$  atm in pressure, and  $2 \times 10^{-9} \text{ g}/\text{cm}^3$  in density ( $\Delta V/V = 10^{-8}$ ).

### EXPERIMENTAL

The apparatus used in these experiments is essentially the same as that used by Lounasmaa.<sup>1</sup> Therefore, it will be described only briefly here. It is shown schematically in Fig. 1.

Helium gas was purified in a trap (not shown) immersed in liquid helium, and was condensed into the piezometer G through the low-temperature valve A, which was kept closed during measurements. G was isolated from the liquid-helium bath by the vacuum case B. Its temperature was controlled by the heater F and by pumping on liquid helium in E.

Changes in the pressure on the sample were measured by the oil manometer K and read with a cathetometer to 0.01 mm, which corresponded to about a millionth of an atmosphere. The absolute pressure was read to 0.01 atm on the Bourdon gauge P, which was calibrated against a dead weight tester. Small changes in the sample density were produced by raising the oil in the left limb of the manometer, forcing gas to condense into G. A change of 0.01 mm in the oil level caused a change of  $2 \times 10^{-9} \text{ g}/\text{cm}^3$  in the density.

Temperatures were measured with a Radiation Research Company Model CG-1 germanium resistance thermometer in a potentiometer circuit using a Honeywell No. 2773 double potentiometer. At the upper lambda point the thermometer resistance was 1483  $\Omega$ , and its sensitivity was 636  $\mu\text{deg}/\Omega$ . With 50  $\mu\text{A}$  of measuring current, the resistance could be measured with a precision of 0.002  $\Omega$ . The measuring current heated the thermometer above the cell temperature, but this effect was reproducible, and the same measuring current was used in calibrating the thermometer. It was calibrated against the vapor pressure of helium in E on the  $T_{58}$  scale,<sup>5</sup> using a tube separate from the pumping tube. The change in the thermometer resistance at the upper lambda point after warming to room temperature and recooling corresponded to a temperature change of less than  $10^{-4} \text{ }^\circ\text{K}$ . All temperatures were referred to the upper lambda point in order to

\* Based on work performed under the auspices of the U. S. Atomic Energy Commission.

<sup>1</sup> O. V. Lounasmaa, Phys. Rev. **130**, 847 (1963).

<sup>2</sup> J. H. Vignos and H. A. Fairbank, Phys. Rev. Letters **6**, 265 and 646 (1961).

<sup>3</sup> E. R. Grilly and R. L. Mills, Ann. Phys. (N. Y.) **18**, 250 (1962).

<sup>4</sup> G. Ahlers, Phys. Rev. **135**, A10 (1964).

<sup>5</sup> H. van Dijk, M. Durieux, J. R. Clement, and J. K. Logan, Nat. Bur. Stds. (U. S.), Monograph 10 (1960).

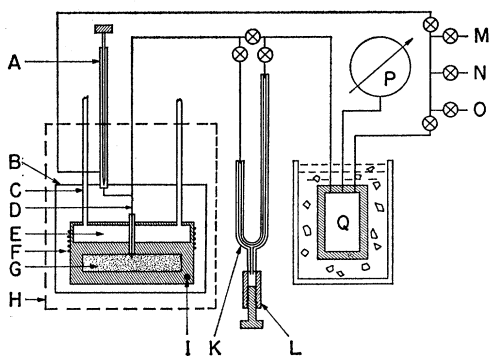


FIG. 1. Schematic drawing of the apparatus. (A) needle valve; (B) vacuum case; (C) pumping and vapor pressure tubes (2) for (E); (D) 30% Cu-Ni capillary tubing, 0.1 mm i.d.; (E) temperature and vapor pressure compartment; (F) heater; (G) piezometer packed with fine copper wire for rapid equilibrium (volume 39.83 cm<sup>3</sup> at 1.76 °K, height 10 mm to keep hydrostatic pressure differences small); (H) dashed lines enclose space immersed in liquid helium bath; (I) germanium thermometer; (K) differential oil manometer, 0.060 in. i.d. constant-bore glass capillary (left arm 40 cm long, right arm 90 cm long); (L) oil reservoir and leveling device filled with Apiezon B oil; (M) to He<sup>4</sup> supply tank and purifier; (N) to pump; (O) to atmosphere; (P) 25-cm dial test gauge calibrated against a dead weight tester; (Q) ballast volume (1461 cm<sup>3</sup>) for balancing the right-hand side of K, held at constant temperature by an ice bath; and ⊗ needle valves.

correct for small changes in the thermometer or the measuring circuit.

For measurements on the melting curve, the sample was cooled below the upper lambda point, and the pressure was raised until freezing began, as indicated by an abrupt rise in temperature. Only a small amount of solid was allowed to form, in order to ensure temperature equilibrium and to avoid blocking of the 0.1-mm capillary D. Then the temperature was raised, and the increase in pressure was read from the manometer. At each temperature no measurements were recorded until equilibrium was established. The sample could not be frozen above the lambda point without blocking the capillaries because of the poorer thermal conductivity of the liquid and the much greater supercooling observed with He I. A few points were obtained by freezing at low temperatures and then warming through the lambda point. Each of these experiments was ended by blocking of the capillary a few millidegrees above the lambda point.

Points on the lambda curve were found by warming the sample slowly at constant volume. Because of the large change in thermal conductivity at the lambda transition, the heating curve showed a sharp break, which could be located to within a microdegree. The sample was held at this temperature until equilibrium was established before reading the manometer. Then the density was changed slightly by raising the oil in the left limb of the manometer, and the new lambda point was found. The break in the heating curve was especially sharp with solid present in the cell, because the heat of melting increased the apparent heat capacity. Thus the upper lambda point could be determined

directly, rather than as the intersection of two independently measured curves.

The pressure coefficient  $\beta_v = (\partial P / \partial T)_v$  was determined by keeping the oil level in the left limb of the manometer constant and measuring the height of oil in the right limb at successively lower temperatures. After the lambda point was passed, as judged by the thermal response, the temperature was raised slowly in order to determine the lambda point exactly.

#### UPPER LAMBDA POINT

A number of absolute determinations of the upper lambda point have been made, since this was used as a reference point for the other measurements. In Table I are listed seven measurements made with different

TABLE I. Determinations of the upper lambda point.

	Temperature °K	Pressure atm
Run No. 9	1.76330	
	1.76330	
	1.76331	
	1.76330	
Run No. 10	1.76324	29.830
	1.76327	29.844
	1.76327	29.834
	1.76333 ± 0.0001	29.84 ± 0.02
Mean	1.763 ± 0.001	
Ahlers (Ref. 4)	1.760 ± 0.001	29.67 ± 0.01
Grilly and Mills (Ref. 3)	1.765 ± 0.003	29.90 ± 0.05
Lounasmaa and Kaunisto (Ref. 6)	1.762 ± 0.001	29.71 ± 0.01
Swenson (Ref. 7)		
(corrected to $T_{88}$ )	1.760 ± 0.003	29.64 ± 0.03

amounts of solid in the cell during the course of two separate cooling runs for which the thermometer calibration was considered especially good. Pressures are listed only for the last run, which immediately preceded the calibration of the pressure gauge.

The absolute accuracy of the temperature measurement was limited by the calibration accuracy, which was estimated to be better than 10<sup>-4</sup> deg relative to the  $T_{88}$  scale. As a check on this, the temperature of the lower lambda point, which is a fixed point on the  $T_{88}$  scale, was measured by the same technique, using the helium in E. The error found in this measurement was 3 × 10<sup>-5</sup> °K.

The absolute pressure measurement was limited by the resolution of the gauge, about 0.01 atm. The gauge calibration is subject to the same error, making the over-all accuracy about 0.02 atm.

Several other recent measurements are listed in Table I. None of the temperature measurements deviates from our value by much more than its estimated error, except for that of Grilly and Mills.<sup>3</sup> But there is additional evidence that the data of Grilly and Mills do not have the precision claimed by them. They find the  $\alpha$ - $\gamma$  solid-phase transition to be at the same temperature as the upper lambda point, whereas Vignos and Fair-

bank<sup>2</sup> and Ahlers<sup>4</sup> have shown that the solid transition is at least 10 mdeg higher.

It is noteworthy that the various lambda-point pressures are in the same numerical order as the corresponding temperatures. It seems likely that all the investigators have measured melting pressures and temperatures accurately but have had varying degrees of success in locating the lambda point. Since we were able to locate the lambda point with a precision of a microdegree and to hold the sample within a micro-degree of the lambda point for long periods of time, we believe our result to be limited only by the absolute accuracy of the thermometer and pressure gauge.

### LAMBDA CURVE

The derivatives  $(dP/dT)_\lambda$ ,  $(d\rho/dT)_\lambda$ , and  $(d\rho/dP)_\lambda$  are shown in Figs. 2 and 3. The solid lines are computed from the equations

$$(dP/dT)_\lambda = -55.54 - 96(T_\lambda - T_{\lambda'}) \text{ atm}/^\circ\text{K}, \quad (1)$$

$$(d\rho/dT)_\lambda = -43.7 - 230(T_\lambda - T_{\lambda'}) \text{ mg/cm}^3 \text{ }^\circ\text{K}, \quad (2)$$

$$(d\rho/dP)_\lambda = 0.7868 + 2.8(T_\lambda - T_{\lambda'}) \text{ mg/cm}^3 \text{ atm}, \quad (3)$$

where  $T_\lambda$  is the lambda temperature for the pressure  $P$  and density  $\rho$ , and  $T_{\lambda'}$  is the temperature of the upper lambda point, 1.7633 °K. The dashed lines are computed by differentiating the cubic equations given by Lounasmaa and Kaunisto.<sup>6</sup> Swenson<sup>7</sup> finds  $-54.5 \text{ atm}/^\circ\text{K}$  for  $(dP/dT)_\lambda$  at  $T_{\lambda'}$ . The agreement is as good as can be expected since Lounasmaa and Kaunisto's measurements were 100 mdeg apart in this region, and Swenson's temperature measurements were not of high enough resolution to permit differentiating his data accurately.

In the case of the density measurements, Lounasmaa

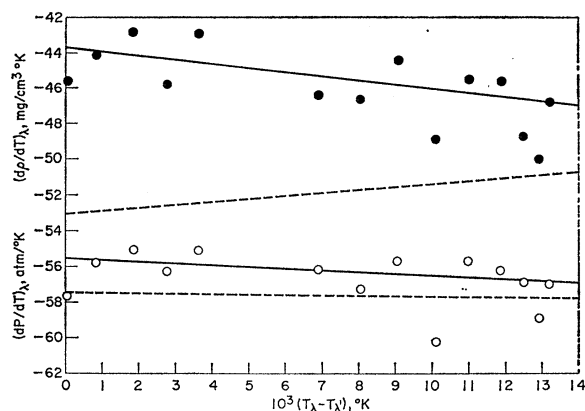


FIG. 2. Derivatives along the lambda curve.  $\circ (dP/dT)_\lambda$ ,  $\bullet (d\rho/dT)_\lambda$ . Solid lines:  $(dP/dT)_\lambda = -55.54 - 96(T_\lambda - T_{\lambda'}) \text{ atm}/^\circ\text{K}$ ;  $(d\rho/dT)_\lambda = -43.7 - 230(T_\lambda - T_{\lambda'}) \text{ mg/cm}^3 \text{ }^\circ\text{K}$ . Dashed lines, Lounasmaa and Kaunisto (Ref. 6).

<sup>6</sup> O. V. Lounasmaa and L. Kaunisto, Ann. Acad. Sci. Fennicae: Ser. A VI, No. 59 (1960); Bull. Am. Phys. Soc. 5, 290 (1960).

<sup>7</sup> C. A. Swenson, Phys. Rev. 89, 538 (1953).

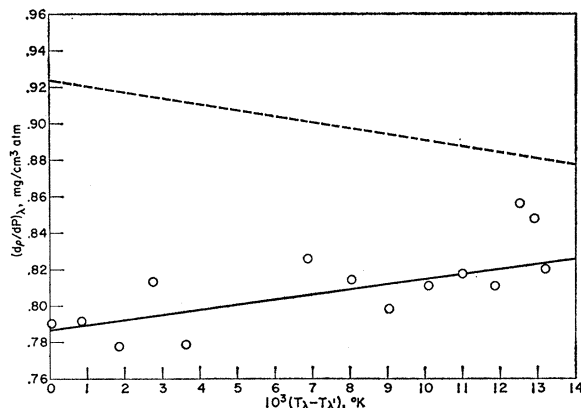


FIG. 3. Derivative  $(d\rho/dP)_\lambda$  along the lambda curve. Solid line:  $(d\rho/dP)_\lambda = 0.7868 + 2.8(T_\lambda - T_{\lambda'}) \text{ mg/cm}^3 \text{ atm}$ ; dashed line, Lounasmaa and Kaunisto (Ref. 6).

and Kaunisto's equation has a curvature (slope of the line in Figs. 2 and 3) of opposite sign from that of our data. It has been pointed out by Goldstein<sup>8</sup> that their equation has an inflection point at 1.87 °K. Our data indicate that the inflection is probably an artifact resulting from fitting a cubic equation to only six experimental points.

These data provide good experimental evidence that the lambda curve is regular at its intersection with the melting curve, as assumed by Goldstein<sup>8</sup> in his discussion of the thermodynamics of the lambda transition. We have, in fact, observed the transition in the supercooled liquid. At a temperature of  $2.4 \times 10^{-5} \text{ }^\circ\text{K}$  below the upper lambda point, we found  $(dP/dT)_\lambda = -56 \text{ atm}/^\circ\text{K}$  and  $(d\rho/dT)_\lambda = -47 \text{ mg/cm}^3 \text{ }^\circ\text{K}$ . This measurement is not as accurate as those in Fig. 2 because of the small temperature interval (He II cannot be supercooled much), but it proves that there is no discontinuity or other irregularity in crossing the melting line.

### MELTING CURVE

In Fig. 4 are plotted measurements of  $(dP/dT)_m$  along the melting curve from 17 mdeg below to 4.3 mdeg above  $T_{\lambda'}$ . The line through the low-temperature points is computed from the equation

$$(dP/dT)_m = 29.43 + 326(T_m - T_{\lambda'}). \quad (4)$$

The points above the lambda transition do not extend to a high enough temperature to define a line, but there does seem to be a change in slope at  $T_{\lambda'}$ .

The Clausius-Clapeyron equation gives, for the slope of the melting curve,

$$(dP/dT)_m = (S_l - S_s)/(V_l - V_s), \quad (5)$$

where  $S_l$ ,  $S_s$ ,  $V_l$ , and  $V_s$  are the molar entropy and volume of liquid and solid, respectively. Differentiating

<sup>8</sup> L. Goldstein, Phys. Rev. 135, A1471 (1964).

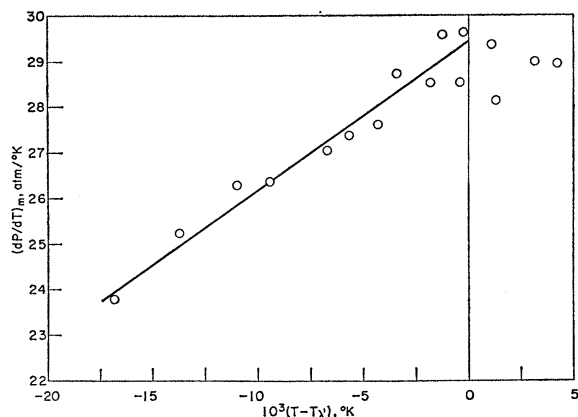


FIG. 4. Derivative  $(dP/dT)_m$  along the melting curve.

with respect to temperature, using (5) and the thermodynamic relations

$$(dS/dT)_m = C_v/T_m + V\alpha[(\partial P/\partial T)_v - (dP/dT)_m], \quad (6)$$

$$(dV/dT)_m = V[\alpha - \kappa(dP/dT)_m], \quad (7)$$

where  $C_v = T(\partial S/\partial T)_v$ ,  $\beta = (\partial P/\partial T)_v = \alpha/\kappa$ ,  $\alpha = V^{-1}(\partial V/\partial T)_p$ , and  $\kappa = -V^{-1}(\partial V/\partial P)_T$ , we find

$$\begin{aligned} (d^2P/dT^2)_m &= (V_l - V_s)^{-1} \\ &\times \{ (C_{vl} - C_{vs})/T_m + V_{\beta l}[(dP/dT)_m - \beta_l]^2 \\ &\quad - V_{\beta s}[(dP/dT)_m - \beta_s]^2 \}. \quad (8) \end{aligned}$$

Ahlers<sup>4</sup> has measured a few values of the heat capacity and compressibility of the gamma solid phase. Both properties are an order of magnitude smaller than those of the liquid, and presumably their variation is small in the neighborhood of the lambda point. Neglecting, then, the terms referring to the solid, we find that the bracketed terms in (8) are all positive, since  $C_v$ ,  $T_m$ ,  $V$ , and  $\kappa$  are necessarily positive and the remaining expression is squared. Now as  $V_l$  is greater than  $V_s$ ,  $(d^2P/dT^2)_m$  must be always positive. It is known<sup>6,9</sup> that  $C_{vl}$  and  $-\beta_l$  (see below) reach very large values at the lambda point and are discontinuous there. The compressibility  $\kappa_l$  is also discontinuous.<sup>1</sup> In all three cases the value is smaller in He I than at the same distance from the lambda point in He II. Hence  $(d^2P/dT^2)_m$  should rise to a large value at the lambda point, drop discontinuously to a smaller value, then continuously to even smaller values, passing through a minimum (but still positive) before rising again as  $C_v$  increases at higher temperatures. Since  $S_l$  and  $V_l$  are continuous,  $(dP/dT)_m$  should have a cusp but no discontinuity. Figure 5 shows schematically how  $(dP/dT)_m$  should behave in the neighborhood of the lambda point, in view of our present knowledge of the qualitative behavior of the other properties.

<sup>9</sup> O. V. Lounasmaa and E. Kojo, Ann. Acad. Sci. Fennicae: Ser. A VI, No. 36 (1959).

Grilly and Mills<sup>3</sup> report the upper triple point, where the  $\alpha$ - $\gamma$  solid-transition line meets the melting curve, to be at the same temperature as the upper lambda point. We would like, first of all, to dispose of the argument that this situation would violate the phase rule by requiring four phases ( $\alpha$ -solid,  $\gamma$ -solid, He I, and He II) to be in equilibrium at  $T_\lambda$ . Because the lambda transition is of the second (or higher) order and has no latent heat, He I and He II are not separate phases in the sense of the phase rule, i.e., two homogeneous regions which have *different physical properties* in equilibrium with each other. He I and He II differ only in the way their properties change as the temperature or pressure moves away from the lambda line.

Grilly and Mills report no change in slope of the melting line at the triple point. This is not thermodynamically possible. As Vignos and Fairbank<sup>2</sup> have pointed out, the discontinuity in slope is given by

$$\begin{aligned} (dP/dT)_{\gamma l} - (dP/dT)_{\alpha l} &= (V_\gamma - V_\alpha)(V_l - V_\gamma)^{-1} \\ &\times [(dP/dT)_{\alpha l} - (dP/dT)_{\alpha \gamma}]. \quad (9) \end{aligned}$$

Substituting Grilly and Mills' values for the volume changes and slopes of the melting curve and the transition line, we find

$$\begin{aligned} (dP/dT)_{\gamma l} - (dP/dT)_{\alpha l} &= (0.201/1.350)(25.3 - 11.6) \\ &= 2.10 \text{ atm/}^\circ\text{K}. \quad (10) \end{aligned}$$

We see no way to reconcile our data with a discontinuity of this magnitude, and we can only conclude that the triple point is outside the range of our measurements. Vignos and Fairbank,<sup>2</sup> who discovered the  $\gamma$  phase, found the upper triple point  $13 \pm 3$  mdeg above the lambda point, and Ahlers<sup>4</sup> found it  $10 \pm 1$  mdeg above the lambda point. We intend to attempt to continue our measurements up to the triple point.

It is difficult to compare our results for  $(dP/dT)_m$  at  $T_\lambda$  with those of other investigators because of the large difference in resolution. Grilly and Mills<sup>3</sup> tabulated melting pressures at 40-mdeg intervals (they did

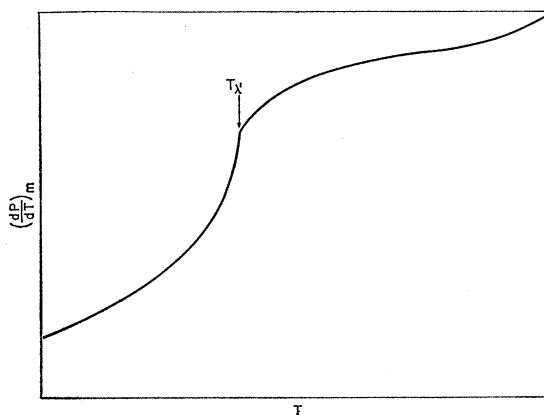


FIG. 5. Qualitative behavior of  $(dP/dT)_m$  in the neighborhood of the lambda point.

not state the interval between *experimental* measurements); hence, they could easily have missed the rise in slope near the lambda point. They reported a slope of 25.3 atm/°K at 1.76 °K (their lambda point) and 19.50 atm/°K at 1.72 °K. We find 29.43 atm/°K at 1.763 °K and 22.91 atm/°K at 1.743 °K. By linear interpolation of Grilly and Mills' values we obtain 22.88 atm/°K at 1.743 °K, so that we agree at 1.743 °K, far from the lambda point. But the second derivative calculated from these two values in their table is only 145 atm/deg<sup>2</sup>, whereas ours is 326 atm/deg<sup>2</sup> [see Eq. (4)].

Similarly, Vignos and Fairbank<sup>2</sup> show only five measurements fairly evenly spaced between 1.7 and 1.765 °K. A rise at the lambda point would not be seen. The slope of their melting curve in this region (scaled from their graph) is about 27 atm/°K.

Swenson<sup>7,10</sup> measured 30 melting pressures between 1.7 °K and the lambda point. He calculated the slopes numerically from carefully smoothed data, and his  $(dP/dT)_m$  curve has the expected shape at the lambda point (which he knew about) but misses completely the triple point (which was not known at that time). This illustrates the danger in smoothing data and probably accounts for his low value for  $(dP/dT)_m$  at  $T_\lambda$ , which was 27.5 atm/°K.

#### PRESSURE COEFFICIENT

The pressure coefficient  $\beta = (\partial P/\partial T)_v$  was measured along an isochore which crossed the lambda line very close to  $T_\lambda$ . Results are shown in Fig. 6, plotted against  $\log_{10}(T - T_\lambda)$ . The equation of the line is

$$\beta_v = 9.39 + 7.69 \log_{10}(T - T_\lambda) \text{ atm/°K}, \quad (11)$$

where  $T_\lambda$  is the lambda transition temperature for the isochore. This graph contains points taken on two different cooling runs. The lambda point for one run

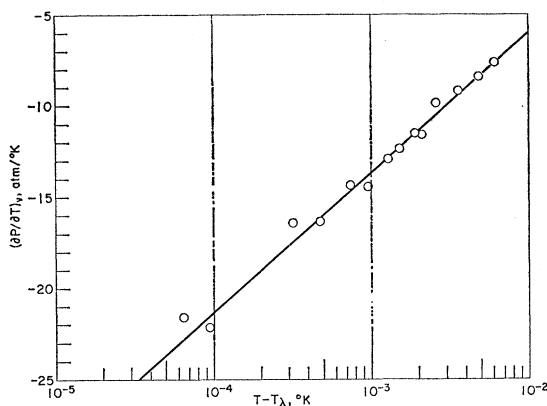


FIG. 6. Pressure coefficient  $\beta_v = (\partial P/\partial T)_v$  of He I along the isochore  $V = V(T_\lambda)$ . Equation of line:  $\beta_v = 9.39 + 7.69 \log_{10}(T - T_\lambda)$  atm/°K.

<sup>10</sup> C. A. Swenson, Phys. Rev. 86, 870 (1952).

was 15  $\mu$ deg below  $T_\lambda$ , and for the other it was 5  $\mu$ deg above. These small differences are not regarded as significant, but the observed lambda point was used in each run in plotting  $T - T_\lambda$ . Since this isochore meets the melting curve at the lambda point, the measurements in Fig. 6 refer to He I. One point was measured in supercooled He II, where  $\beta_v$  was found to be  $-27.6$  atm/°K at  $T - T_\lambda = -1.08 \times 10^{-5}$  °K. This point is not plotted in Fig. 6, but it is approximately the value to be expected for  $T - T_\lambda = 1.08 \times 10^{-5}$  °K.

At the lambda line, it is easily shown that

$$\beta_v = (\partial P/\partial T)_v = (dP/dT)_\lambda - (\rho\kappa)^{-1}(d\rho/dT)_\lambda. \quad (12)$$

This equation should apply to any point close enough to the lambda line so that  $\beta_v$  and  $\kappa$  depend only on the distance from the lambda line. Now solving for  $\rho\kappa$  we have

$$\rho\kappa = \left( \frac{\partial \rho}{\partial P} \right)_T = \frac{(d\rho/dT)_\lambda}{(dP/dT)_\lambda - \beta_v}, \quad (13)$$

from which  $\rho\kappa$  can be calculated for points on the isochore along which we measured  $\beta_v$ . Some calculated values are given in Table II. If  $\beta_v$  becomes equal to

TABLE II. Calculated values of  $(\partial \rho/\partial P)_T$  of He I for points  $(T, P)$  on the isochore terminating at the upper lambda point  $(T_\lambda, P_\lambda)$ .  $P_\lambda$  is the lambda point pressure at the temperature  $T$ .

$T - T_\lambda$ , °K	$10^3(P_\lambda - P)$ atm	$10^3(P - P_\lambda)$ atm	$(\partial \rho/\partial P)_T$ mg/cm <sup>3</sup> atm
$5 \times 10^{-6}$	0.1735	0.1042	1.807
$10^{-5}$	0.3238	0.2316	1.649
$5 \times 10^{-5}$	1.351	1.426	1.371
$10^{-4}$	2.470	3.084	1.278
$5 \times 10^{-4}$	9.662	18.11	1.105
$10^{-3}$	17.01	38.53	1.044
$5 \times 10^{-3}$	58.19	219.5	0.925

$(dP/dT)_\lambda$  at the lambda point, then  $\kappa$  must become infinite there. However, since  $\beta_v$  is much smaller in magnitude than  $(dP/dT)_\lambda$ , even at  $T - T_\lambda = 10^{-6}$  °K, it will be difficult to observe an anomaly in  $\kappa$ .

The logarithmic dependence of  $\beta_v$  on  $T - T_\lambda$  is similar to that found by Lounasmaa<sup>1</sup> and by Lounasmaa and Kaunisto<sup>6</sup> at lower densities, and is consistent with their observation that the two constants in Eq. (11) both increase with increasing density. At a constant small value of  $T - T_\lambda$ ,  $\beta_v$  increases in magnitude with increasing density, whereas its limiting value, the slope of the lambda curve, decreases in magnitude with increasing density. For example, at  $T - T_\lambda = 10^{-6}$  °K, which is probably the limit of temperature resolution now attainable,  $\beta_v$  at the upper lambda point is  $-36.75$  atm/°K according to (11), compared to  $-55.54$  atm/°K for  $(dP/dT)_\lambda$ . In Lounasmaa's experiment<sup>1</sup> at  $\rho = 0.1654$  g/cm<sup>3</sup> and  $T_\lambda = 2.023$  °K,  $\beta_v = -16.9$  atm/°K and  $(dP/dT)_\lambda = -75.86$  atm/°K. This shows the great

advantage, in investigating the nature of the lambda transition, of working near the upper lambda point.

Goldstein<sup>8</sup> has pointed out that it is meaningless to extrapolate equations like (11) to values of  $T - T_\lambda$  which are less than the root-mean-square statistical temperature fluctuation, which is about  $10^{-12}$  °K for Lounasmaa's experiments<sup>1,6</sup> as well as the present one. In the experiment<sup>1</sup> at  $\rho = 0.1654$ , if the logarithmic equation is extrapolated to  $T - T_\lambda = 10^{-12}$  °K,  $\beta_v$  is still not one half of its limiting value  $(dP/dT)_\lambda$ ; whereas in our experiment Eq. (11) predicts that  $\beta_v$  will reach its limiting value at  $T - T_\lambda = 3.5 \times 10^{-9}$  °K, well outside the range of statistical fluctuations. It is even possible

that a resolution of  $10^{-9}$  °K may sometime be achieved experimentally.

#### ACKNOWLEDGMENTS

The author wishes to express his indebtedness to Professor O. V. Lounasmaa of the Institute of Technology, Helsinki, who originally constructed the apparatus and has contributed valuable advice; to Professor Dillon Mapother of the University of Illinois for fruitful discussions during the progress of the work; and to S. T. Picraux and Zenon Sungaila for assistance in modifications to the apparatus.

## Nonlinear Optical Properties of Liquids

J. A. GIORDMAINE

*Bell Telephone Laboratories, Murray Hill, New Jersey*

(Received 28 January 1965)

Nonlinear optical polarization quadratic in the optical electric fields is shown to occur in optically active liquids and to lead to sum- and difference-frequency generation; second-harmonic generation is forbidden. The nonlinearity is described by components of the second-order polarizability tensor  $\chi_{ijk}$  antisymmetric in  $j$  and  $k$ ; the form of the antisymmetric part of  $\chi_{ijk}$  is given for all the crystal classes and textures and for isotropic media. The magnitude of nonlinear polarizability of liquids is estimated from second-order perturbation theory and calculated to be readily detectable in many optically active liquids. The mechanism of the nonlinearity is illustrated by a simple single-electron molecular model.

### I. INTRODUCTION

IT has been shown by Franken *et al.*<sup>1</sup> that in crystals without a center of symmetry one can observe optical polarization quadratic in the applied optical electric field. Radiation from this nonlinear polarization leads to generation of second harmonics and sum and difference frequencies. It is now possible to convert over 20% of a laser beam into new frequencies through this effect.<sup>2</sup> Bloembergen *et al.*,<sup>3</sup> Kleinman,<sup>4</sup> and others<sup>5</sup> have given theoretical analyses of the effect.

The second-order nonlinearities have been studied in a variety of piezoelectric crystals, primarily by observation of second-harmonic generation.<sup>6</sup> Higher order nonlinearities have also been observed in centrosymmetric media, including calcite<sup>7,8</sup> and several liquids.<sup>9</sup>

Some of the higher order effects arise from magnetic-dipole and quadrupole interactions and lead to very weak second-harmonic generation and mixing; higher order electric-dipole effects produce weak third harmonics as well as other nonlinear effects. In this paper, we shall consider only electric-dipole-type nonlinearities of second order which produce in noncentrosymmetric materials a macroscopic polarization quadratic in the applied fields.

The tensor  $\chi_{ijk}^{2\omega, \omega, \omega}$  relating the polarization  $P_i^{2\omega}$  to the applied fields  $E_j^\omega$  and  $E_k^\omega$  in second-harmonic generation is inherently symmetric in the indices  $j$  and  $k$ . This symmetry expresses the fact that fields  $E$  and  $E'$  applied, respectively, along the  $x$  and  $y$  axes, for example, produce the same quadratic polarization as the fields  $E$  and  $E'$  applied along the  $y$  and  $x$  axes, since the fields are indistinguishable. The tensor  $\chi_{ijk}^{2\omega, \omega, \omega}$  must therefore have the same form for the various crystallographic classes as the piezoelectric tensor relating electric polarization to the stress, a symmetric

<sup>1</sup> P. A. Franken, A. E. Hill, C. W. Peters, and G. Weinreich, *Phys. Rev. Letters* **7**, 118 (1961).

<sup>2</sup> R. W. Terhune, P. D. Maker, and C. M. Savage, *Appl. Phys. Letters* **2**, 54 (1963).

<sup>3</sup> J. A. Armstrong, N. Bloembergen, J. Ducuing, and P. S. Pershan, *Phys. Rev.* **127**, 1918 (1962).

<sup>4</sup> D. A. Kleinman, *Phys. Rev.* **128**, 1761 (1962).

<sup>5</sup> P. S. Pershan, *Progress in Optics*, edited by E. Wolf (North-Holland Publishing Company, Amsterdam, 1965, to be published).

<sup>6</sup> R. C. Miller, *Appl. Phys. Letters* **5**, 17 (1964).

<sup>7</sup> R. W. Terhune, P. D. Maker, and C. M. Savage, *Phys. Rev. Letters* **8**, 404 (1962).

<sup>8</sup> J. A. Giordmaine, *Proceedings of the Third Conference on*

*Quantum Electronics, Paris, 1963*, edited by P. Grivet and N. Bloembergen (Columbia University Press, New York, 1964), p. 1549.

<sup>9</sup> P. D. Maker, R. W. Terhune, and C. M. Savage, *Proceedings of the Third Conference on Quantum Electronics, Paris, 1963*, edited by P. Grivet and N. Bloembergen (Columbia University Press, New York, 1964), p. 1559.